Available online at www.sciencedirect.com
ScienceDirect
Biosensors and Bioelectronics 23 (2007) 485–491
BIOSENSORS & BIOELECTRONICS
www.elsevier.com/locate/bios

Successively amplified electrochemical immunoassay based on biocatalytic deposition of silver nanoparticles and silver enhancement

Zhao-Peng Chen [a,b], Zhao-Feng Peng [a], Yan Luo [a], Bo Qu [c], Jian-Hui Jiang [a], Xiao-Bing Zhang [a], Guo-Li Shen [a], Ru-Qin Yu [a,*]

[a] *State Key Laboratory for Chemo/Biosensing and Chemometrics, College of Chemistry and Chemical Engineering, Hunan University, Changsha 410082, China*
[b] *Department of Environmental Chemistry, Yantai Institute of Coastal Zone Research for Sustainable Development, Chinese Academy of Sciences, Yantai 264003, China*
[c] *Chemistry and Chemical Engineering College, Key Laboratory of Chemical Biology and Traditional Chinese Medicine Research (Ministry of Education), Hunan Normal University, Changsha 410081, China*

Received 11 February 2007; received in revised form 29 May 2007; accepted 22 June 2007
Available online 20 July 2007

Abstract

A successively signal-amplified electrochemical immunoassay has been reported on the basis of the biocatalytic deposition of silver nanoparticles with their subsequent enlargement by nanoparticle-promoted catalytic precipitation of silver from the silver-enhancer solution. The immunoassay was carried out based on a heterogeneous sandwich procedure using polystyrene microwells to immobilize antibody. After all the processes comprising the formation of immunocomplex, biocatalytic deposition of silver nanoparticles and following silver enhancement were completed, the silver on polystyrene microwells was dissolved and quantified by anodic stripping voltammetry (ASV). The effect of relevant experimental conditions, including the concentration of ascorbic acid 2-phosphate (AA-p) substrate and Ag(I) ions, the biocatalytic deposition time, and of crucial importance, the silver enhancement time, were investigated and optimized. The anodic stripping peak current was proportional to the concentration of human IgG in a dynamic range of 0.1–10 ng ml^{-1} with a detection limit of 0.03 ng ml^{-1}. Scanning electron microscope (SEM) was applied to characterize the silver nanoparticles before and after silver enhancement on the surface of polystyrene microplates. By coupling the highly catalytic effect of enzyme and nanoparticles to successively amplify the analytical signal, the sensitivity of immunoassay was enhanced so dramatically that this approach would be a promising strategy to achieve a lower detection limit for bioassays.

Keywords: Electrochemical immunoassay; Biocatalytic deposition; Silver nanoparticles; Silver enhancement; Anodic stripping voltammetry

1. Introduction

There is an increasing demand for ultrasensitive methods of immunoassay based on the specific recognition of antigen to be detected by corresponding antibody. Among many analytical techniques, electrochemical detections are very attractive for such bioassays due to its unique advantages such as high sensitivity, intrinsic simplicity, field portability and inexpensive instrumentation. As the quantification in immunoassay or DNA assays is generally achieved by measuring the specific activity of a label, enzymes and nanoparticles used as labels play a vital role in the development of signal-amplified electrochemical bioaffinity assays of proteins and nucleic acids (Bakker and Telting-Diaz, 2002; Bakker, 2004; Bakker and Qin, 2006; Wang, 1999; Katz et al., 2004).

Enzyme-linked immunosorbent assay (ELISA) is widely applied for the determination of proteins. Traditionally, the second antibody is conjugated with enzyme that catalyzes a reaction with color change, which can be detected photometrically. However, the low sensitivity of this immunoassay limits its further application in practical, clinical, and environmental analysis. In recent years, new schemes based on coupling the biocatalytic

* Corresponding author. Tel.: +86 731 8822577; fax: +86 731 8821355.
E-mail address: rqyu@hnu.cn (R.-Q. Yu).

0956-5663/$ – see front matter © 2007 Elsevier B.V. All rights reserved.
doi:10.1016/j.bios.2007.06.005

amplification of enzyme labels with additional electrochemical detections have been developed for meeting the demands of highly sensitive bioassays. Willner's group reported on the use of chronopotentiometry and Faradaic impedance spectroscopy for the detection of the biocatalytic precipitative accumulation of the insoluble reaction product on gold electrode surface (Katz et al., 2001; Alfonta et al., 2001). The application of carbon nanotubes (CNTs) as a dual amplification role both in the recognition process for loading numerous enzyme labels and in the transduction events for accumulating the product of enzymatic reaction was proposed to dramatically amplify enzyme-based bioaffinity electrochemical sensing of proteins and DNA (Wang et al., 2004). Hwang et al. (2005) developed a DNA sensor based on chemical accumulation of silver metal as an enzyme-catalyzed reduction product, a process termed as biometallizaion by the author, to achieve multiple amplifications and very low detection limits. Because the electro-active metallic product accumulates on the electrode during the enzymatic reaction, preventing the diffusing out of the enzyme-catalyzed product into the solution, the coupling of enzyme catalysis with metal deposition seems to be a promising strategy for highly sensitive bioaffinity assay.

Metal nanoparticles as a class of labels with many unique features such as optical, electronic, magnetic, and catalytic properties have been explored for potential applications in biomolecular detection (Katz et al., 2004). Based on these advantages, colloidal gold was first applied as TEM marker in 1971 (Faulk and Taylor, 1971), and was then introduced for SEM in 1975 (Horisberger et al., 1975). Recently, besides the application of metal nanoparticles in some analytical methods such as UV–vis (Schofield et al., 2006), Raman (Ni et al., 1999; Santos et al., 2004) and time-resolved fluorescence spectroscopy (Ipe and Thomas, 2004), SPR (He et al., 2000; Lyon et al., 1998) or QCM techniques (Zhou et al., 2000), a new electrochemical metalloimmunoassay by using colloidal gold as label was reported, which pushed the sensitivity of immunoassay to the picomolar domain (Dequaire et al., 2000). Further sensitivity enhancement can be obtained by the application of metal-enhanced gold nanoparticles, where functional gold nanoparticles act as catalysts to reduce gold or silver ions on themselves. Based on this principle, Mirkin's group has developed a scanometric DNA array (Taton et al., 2000), an electrical detection-based DNA array (Park et al., 2002) and Raman spectroscopic fingerprints for DNA and RNA detection (Cao et al., 2002). In these methods, the autocatalytic metal deposition procedure enlarges the size and darkens the color of nanoparticles, resulting in two to three orders of magnitude improvement in detection sensitivity of scanning electrochemical microscope (Wang et al., 2002), QCM (Su et al., 2001) or electrochemical stripping techniques (Wang et al., 2001; Cai et al., 2002; Liao and Huang, 2005; Chu et al., 2005). Anodic stripping voltammetry (ASV) has been proved to be a powerful approach for trace determination of metal ions (Jacobs, 1963; Dequaire et al., 2000). Its remarkable sensitivity is attributed to the preconcentration step during which the target metal is accumulated onto the surface of the working electrode through cathodical electro-deposition and the stripping step when the metal is stripped from the electrode by anodic oxidation. Such association of nanoparticle-promoted metal precipitation with the remarkable sensitivity of stripping metal analysis offers a dramatic enhancement of the signal response of immunoassay and DNA assays.

In this paper, a successively amplified electrochemical immunoassay is presented for the detection of human IgG based on coupling the biocatalytic deposition of silver nanoparticles with subsequent silver enhancement. As one of the most important enzymatic labels for ELISA due to its high turnover number and broad substrate specificity, alkaline phosphatase (ALP) was adopted to be the indicator for the analyte by using ascorbic acid 2-phosphate (AA-p) as substrate, which has been proved feasible for electrochemical detection (Kokado et al., 2000). After the sandwich type immunocomplex was formed, the ALP bound on the polystyrene microwells converted the AA-p into ascorbic acid. The latter, in turn, reduced the Ag(I) ions in the solution, leading to the deposition of a layer of yellow silver nanoparticles onto the surface of polystyrene microwells. These deposited silver nanoparticles subsequently catalyzed the spontaneous reaction of Ag(I) ions and hydroquinone in the silver-enhancer solution, resulting in the deposition of silver metal onto the particle surface and further enlargement of the size of nanoparticles, which are dissolved by HNO_3 and quantified by ASV. SEM was also utilized to characterize the silver nanoparticles formed. The successive amplification strategy provides a promising way for improving the sensitivity of electrochemical immunoassay as applied to biosensing.

2. Experimental

2.1. Materials and reagents

Goat anti-human IgG antibody, human IgG, and bovine serum albumin (BSA) were purchased from Beijing Dingguo Biotechnology Development Center (Beijing, China). Alkaline phosphatase (ALP) conjugated goat anti-human IgG antibody was provided by Beijing Zhongshan Biotechnology Reagents. Ascorbic acid 2- phosphate (AA-p) was obtained from Express Technology Co. Ltd. (Japan).

Buffers used in this study included 0.05 M $NaHCO_3$–Na_2CO_3 (pH 9.6) as coating medium and 0.05 M sodium phosphate-buffered saline (PBS, pH 7.4) as incubating and washing buffer. The enzyme reaction solution was a glycine–NaOH buffer containing 1.5 mM AA-p and 1 mM $AgNO_3$ (pH 9.0), while the silver-enhancer solution was a citrate buffer containing 2.0 mM $AgNO_3$ and 4 mg ml^{-1} hydroquinone (pH 3.5). Other reagents were of analytical purity, and ultra pure water of specific resistance 18 MΩ was used throughout the experiments.

2.2. Apparatus

Electrochemical measurements were performed with a three-electrode system comprising a carbon paste electrode (CPE) as working electrode, a saturated calomel electrode (SCE) as reference electrode, and a platinum wire as auxiliary electrode. The solid CPE was prepared by mixing the graphite (1.0 g) and melted paraffin (0.5 g) into a homogeneous paste and then

filling it into the Teflon tube (4.5 mm inner diameter). All of the electrochemical experiments were implemented on CHI660 electrochemical workstation (Shanghai Chenhua Instruments, Shanghai, China).

The Scanning electron microscope (SEM) photographs were taken by a JEOL JSM-6700F field emission scanning electron microscope. The basic experimental parameters such as imaging mode (secondary electron), accelerating voltage, magnification and working distance (WD) were labeled on each figure.

2.3. Immunoassay procedure

The principle of heterogeneous electrochemical immunoassay applied to quantify human IgG analyte is depicted in Scheme 1. First, 100 μl of 0.25 mg ml^{-1} goat anti-human IgG antibody dissolved in 0.05 M $NaHCO_3$–Na_2CO_3 buffer was added to the polystyrene microwells and incubated at 4 °C overnight. After removing the solution, the wells were rinsed with 0.05 M PBS for eight times, a repeated process executed after each following step until the enzyme reaction. Then 150 μl of 1% BSA solution (dissolved in 0.05 M PBS) was injected to block the active sites of the wells at 37 °C for 1 h. After that, 100 μl of different concentration of human IgG standard solutions were added into the wells and incubated at 37 °C for another 1 h. Following this step, 100 μl of ALP-conjugated antibody was injected at 37 °C for an additional hour. After the formation of the sandwich immunocomplex, the wells were rinsed with 0.05 M PBS for four times and ultra pure water for four times. Subsequently 100 μl of enzyme reaction solution was added into the wells, on which silver nanoparticles was deposited at 37 °C for 15 min. After removing the solution and rinsing the wells with ultra pure water for four times, 100 μl of the silver-enhancer solution was added and incubated at 25 °C for another 15 min.

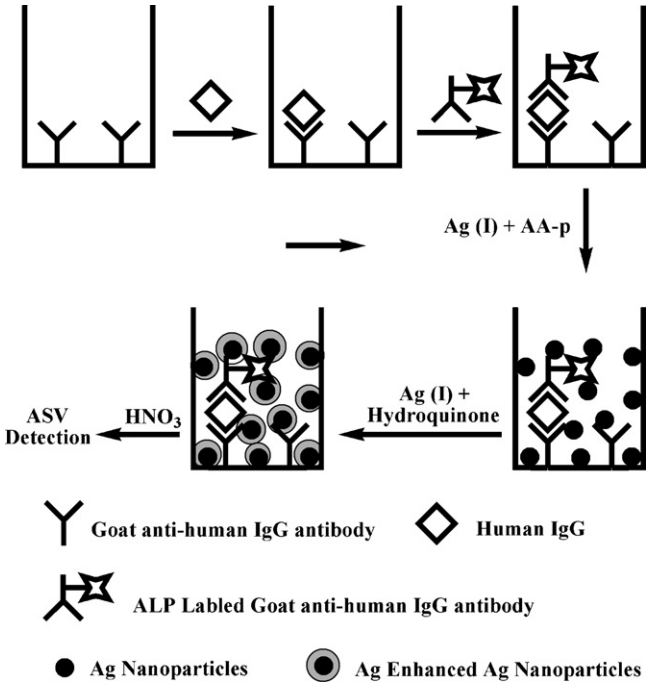

Scheme 1. Schematic presentation of the immunoassay procedure.

Finally, the deposited silver was dissolved by 100 μl of 5 M HNO_3 and then quantified by ASV as described in the following section.

2.4. Electrochemical determination

After the silver on the microwells was completely dissolved, the solution was transferred from microwells into the electrolytic cells, and appropriate amount of KNO_3 solution (0.1 M) was added into the cells to achieve a final volume of 5 ml. The ASV was carried out in the electrolytic cells using the aforementioned three-electrode system. Before each determination, the carbon paste electrodes were polished on a sheet of printing paper to obtain a renewable surface. The reference electrode (SCE) was separated from the detection solution that contains Ag(I) ions in the electrolytic cells by a glass salt bridge of saturated KNO_3 solution, in order to avoid the interference caused by the continuous leaching of chloride anion that lead to AgCl precipitation. The ASV experimental parameters to quantify Ag(I) ions were investigated and optimized: an electro-deposition time of 10 min and deposition potential of −0.5 V were adopted and the current signal was recorded from −0.2 to 0.7 V at a scan rate of 100 mV s^{-1} according to our previous work (Chu et al., 2005). Under the optimal conditions selected above, the sensitive ASV determination of Ag(I) ions at a carbon paste electrode (detection limit was 1×10^{-8} M based on the 3σ-rule, where σ is the standard deviation of a blank solution, $n = 6$) further warranting the high performance of the immunoassay method.

3. Results and discussion

3.1. SEM characterization

Since it is the first application in the field of nanoparticles (Horisberger et al., 1975), SEM has become a powerful technique to detect the exterior state of samples. In this work, SEM was applied to characterize the silver nanoparticles before and after silver enhancement on the surface of polystyrene microplates. The preparation process of the samples was the same as described above, only the polystyrene microwells were replaced by polystyrene microplates for the requirement of SEM analysis.

Fig. 1 displays the silver nanoparticles deposited on the surface of polystyrene microplates before silver enhancement with a biocatalytic deposition time of 10 min (a) and 20 min (b). The size of silver nanoparticles in both cases was 20–30 nm, showing no enlargement with the increase of the biocatalytic deposition time. Some bigger particles in the figures are possibly caused by the aggregation of the silver nanoparticles, a phenomenon unavoidable with the exposure of nanoparticles to the air before SEM analysis. It can be assumed that more biocatalytic deposition time would result in the increase of the quantity of silver nanoparticles rather than the enlargement of the particles already formed, which was advantageous to the following silver enhancement. This assumption was subsequently confirmed by electrochemical experiments.

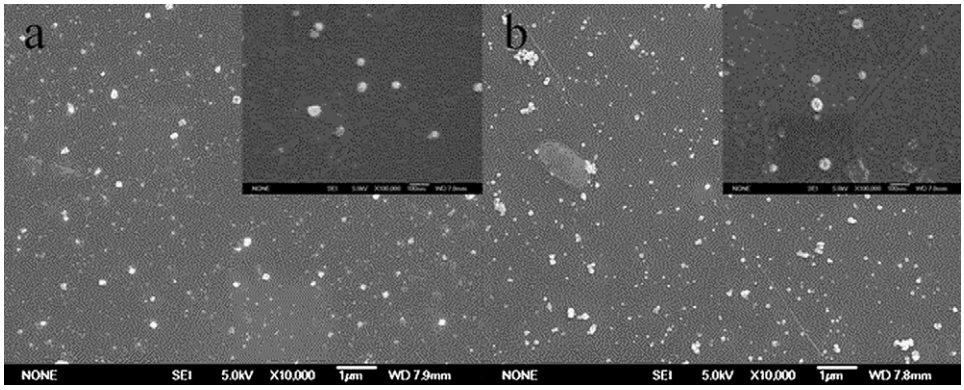

Fig. 1. The SEM images of the silver nanoparticles before silver enhancement with a biocatalytic deposition time of 10 min (a) and 20 min (b). The images were taken at a magnification of 10k while the insets were taken on the same sample at a magnification of 100k.

The images of the silver nanoparticles after silver enhancement are illustrated in Fig. 2 with a biocatalytic deposition time of 20 min and a silver enhancement time of 10 min (a), 20 min (b) and 30 min (c), respectively. It is perceptible that within the first 10 min, the silver enhancement reaction was very slow as though the manifestation of the catalytic effect of the silver nanoparticles as crystal nucleus requires some induction period. When silver enhancement time reached 20 min, the nanoparticle-promoted silver precipitation became significant accompanied with the enlargement of nanoparticles, the size of silver nanoparticles was approximately 50–60 nm and the volume was approximately 20 times larger than that before the silver enhancement. After 30 min, the silver enhancement reaction tended to be complete, when the size of nanoparticles enlarges to nearly 100 nm. These phenomena of the nanoparticles enlargement were further confirmed by the electrochemical experiments in the following part.

3.2. Optimization of the immunoassay conditions

3.2.1. Effect of the AA-p concentration

Since the amount of biocatalytically deposited silver nanoparticles is dependent on the amount of ascorbic acid generated by enzyme-catalytic reaction, which is controlled by the concentration of AA-p substrate, the effect of the AA-p concentration on the quantity of deposited silver nanoparticles was investigated. As shown in Fig. 3a, after a biocatalytic deposition for 20 min in the glycine–NaOH buffer containing 1 mM $AgNO_3$ and varying concentration of AA-p, the anodic stripping current of silver for the determination of 1 $\mu g\,ml^{-1}$ human IgG increases with the concentration of AA-p up to 1.5 mM, and then tended to stabilize. As a result, an AA-p concentration of 1.5 mM was adopted in the subsequent study.

3.2.2. Effect of the Ag(I) ions concentration

The amount of biocatalytically deposited silver nanoparticles is also dependent on the concentration of Ag(I) ions in the enzyme reaction solution. Sufficient Ag(I) ions should be added to it in order to prevent the diffusion of enzyme-generated ascorbic acid, ensuring that the ascorbic acid was oxidized as soon as it was produced on the surface of the microwells. Thus, the effect of the Ag(I) ions concentration on the stripping current was also investigated. As shown in Fig. 3b, with a biocatalytic deposition time of 20 min in the glycine–NaOH buffer containing 1.5 mM AA-p and varying concentration of $AgNO_3$, the anodic stripping current for the determination of 1 $\mu g\,ml^{-1}$ human IgG increases with the concentration of Ag(I) ions from 0.2 to 1.0 mM, after that it began to level off. It seems that high concentration of Ag(I) ions could deactivate the enzyme, reflecting on the decreasing efficiency of the biocatalytic deposition. As a result, an Ag(I) ions concentration of 1.0 mM was selected in the following experiments.

3.2.3. Effect of the biocatalytic deposition time

Apparently the quantity of deposited silver nanoparticles is related to the biocatalytic deposition time. Admittedly, more deposition time results in more deposited silver nanoparticles, but the immunoassay time would also be extended. Hence, the

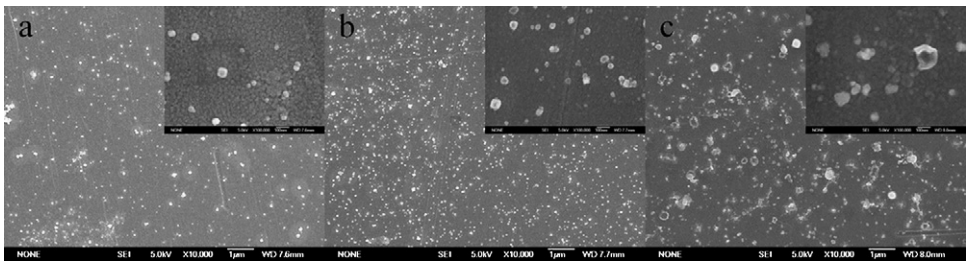

Fig. 2. The SEM images of the silver nanoparticles after silver enhancement with a biocatalytic deposition time of 20 min and a silver enhancement time of 10 min (a), 20 min (b), and 30 min (c). The images were taken at a magnification of 10k while the insets were taken on the same sample at a magnification of 100k.

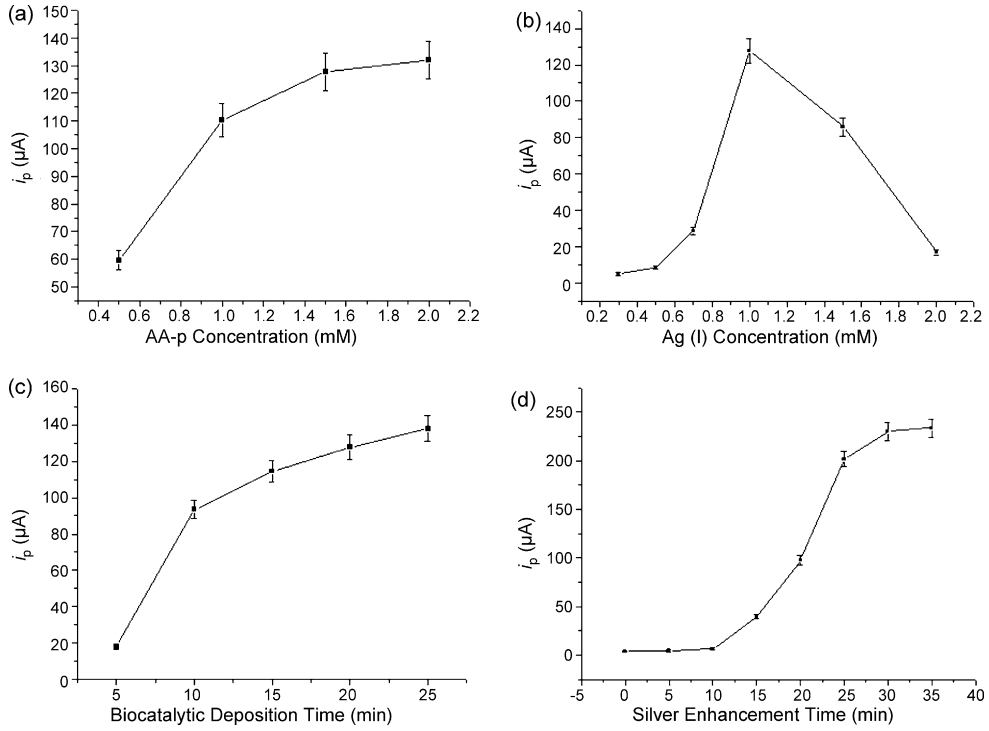

Fig. 3. The effect of the (a) concentration of AA-p, (b) concentration of Ag(I) ions, (c) biocatalytic deposition time, and (d) silver enhancement time on the stripping peak current. Error bars represents S.D. and $n = 4$.

biocatalytic deposition time was optimized as follows: after reacting in the glycine–NaOH buffer containing 1.5 mM AA-p and 1.0 mM $AgNO_3$ for different times, the deposited silver nanoparticles was quantified for the determination of 1 μg ml^{-1} human IgG. Fig. 3c reveals that the anodic stripping current ascended with the increase of the biocatalytic deposition time before 15 min, and then inclined to be stable. This phenomenon implies that the enzyme reaction rate has greatly decreased over 15 min along with the deactivation of enzyme. As a result, a biocatalytic deposition time of 15 min was accepted in the subsequent work.

3.2.4. *Effect of the silver enhancement time*

A citrate buffer containing 2.0 mM $AgNO_3$ and 4 mg ml^{-1} hydroquinone (pH 3.5) was adopted as the silver-enhancer solution. This solution was chosen according to the following reasoning. When the concentration of silver-enhancer solution is too high, the silver enhancement time would be too short (in several seconds) to be controllable. All of the Ag(I) ions in the silver-enhancer solution were almost reduced into silver metal in such a fleeting time that made the immunoassay difficult to be proceeding. If the concentration were too low, the extended time of silver enhancement would result in the unfavorable immunoassay time (over an hour).

When the concentration of silver-enhancer solution was set, the silver enhancement time should also be optimized. It can be predicted that less silver enhancement time would lead to smaller signal amplification, which has a critical effect on the sensitivity of immunoassay. On the other hand, more silver enhancement time would prolong the analytical time and, more seriously, result in the enhancement of the background signal, which highly decreases the signal–noise ratio of the immunoassay. One can see in Fig. 3d that the silver enhancement reaction was extremely slow during the first 10 min. After that, along with the continual enlargement of the silver nanoparticles on polystyrene microwells, the nanoparticle-promoted reaction that catalyzed the reduction of Ag(I) ions by hydroquinone became more and more rapid. However, as the Ag(I) ions in the silver-enhancer solution were almost reduced on the silver nanoparticles after 25 min, the signals for the determination of 10 ng ml^{-1} human IgG tend to be stable. Therefore, a silver enhancement time of 15 min was selected in order to achieve ultrasensitivity, with this time period the signal amplification was approximately 10 times as illustrated in Fig. 4.

3.3. *Analytical performance for determination of human IgG*

The principle of immunoassay was described above. After the immunocomplex was formed on the surface of polystyrene microwells, the ALP catalyzed the hydrolysis of AA-p to ascorbic acid, a reagent that could reduce the Ag(I) ions in the solution. Because the half-wave potential of ascorbic acid is 0.39 V versus NHE and that of Ag(I) ions is 0.7995 V, the ascorbic acid in alkaline solution would spontaneously reduce Ag(I) ions. The hydrolysis and reducing reaction can be described as follows

$$\text{ascorbic acid 2-phosphate} \xrightarrow[\text{pH 9.0}]{\text{ALP}} \text{ascorbic acid} + H_3PO_4$$

$$\text{ascorbic acid} + 2Ag^+ \rightarrow \text{dehydroascorbic acid} + 2H^+ + 2Ag$$

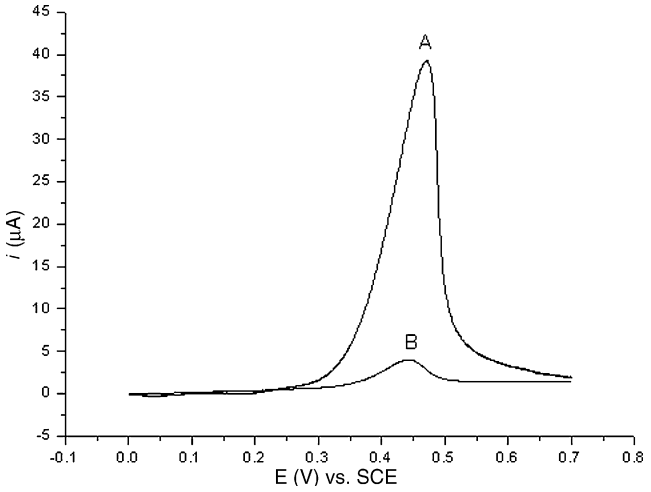

Fig. 4. The anodic stripping voltammograms before (b) and after (a) silver enhancement.

After incubated at 37 °C for 15 min, a layer of yellow silver nanoparticles was deposited onto the surface of polystyrene microwells. Silver nanoparticles have such high surface-to-volume ratio that they could act as crystal nucleus to catalyze the reaction of Ag(I) ions and hydroquinone, a very slow reaction without the catalysts. That the Ag(I) ions in the silver-enhancer solution were reduced by hydroquinone to silver metal at the surfaces of silver nanoparticles resulted in the deposition of more silver on the microwells. Coupled with the anodic stripping metal analysis, the sensitivity of immunoassay was dramatically enhanced, achieving a relatively lower detection limit.

In addition, 1% BSA was selected to replace human IgG in the process of sandwich immunoreactions for the purpose of investigating the effect of non-specific adsorption. Its stripping peak current was 3.8 μA (S.D. = 0.70 μA and $n = 6$). Compared with the signal for the determination of 10 ng ml^{-1} human IgG (40 μA, S.D. = 2.5, and $n = 4$), this background caused by non-specific adsorption was so low that the immunoassay had relatively good selectivity without the interference of non-specific adsorption.

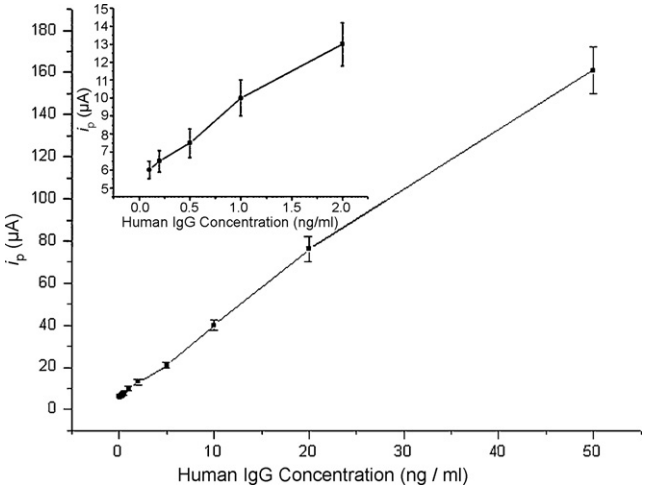

Fig. 5. The calibration curve for the detection of human IgG, indicating that the stripping peak current plotted vs. the concentration of human IgG. The low concentration was reproduced more distinctly in the inset. Error bars represents S.D. and $n = 4$.

When the concentration of human IgG was enhanced, the amount of ALP bound on the polystyrene microwells increased correspondingly, resulting in multiplication of the biocatalytically deposited silver nanoparticles subsequently enlarged by silver metal reduced from the silver-enhancer solution. It can be observed in Fig. 5 that the stripping peak current as analytical signal was proportional to the concentration of human IgG as the analyte in the dynamic range of 0.1–50 ng ml^{-1}, The linear regression equation was i_p (μA) = 5.88 + 3.27C (human IgG concentration), with a correlation coefficient of 0.9972. The signal saturated above 50 ng ml^{-1} human IgG, possibly because nearly all of the Ag(I) ions in the silver-enhancer solution had been reduced. As calculated by the 3σ-rule (where σ is the standard deviation of a blank solution and $n = 6$), the detection limit was 0.03 ng ml^{-1}, which is approximately 67 times more sensitive than that (2 ng ml^{-1}) before silver enhancement.

4. Conclusion

A successively amplified electrochemical immunoassay is proposed for the determination of human IgG based on the biocatalytic deposition of silver nanoparticles and subsequent silver enhancement, which was characterized by SEM and quantified by electrochemical assays. The coupling of the high catalytic action of enzyme and metal nanoparticles makes the immunoassay ultrasensitive with a very low detection limit, favorably compared with the electrochemical metalloimmunoassay based on a colloidal gold label of which detection limit for goat IgG is 0.5 ng ml^{-1} (Dequaire et al., 2000). This strategy is even preferable to the electrochemical stripping metalloimmunoassay based on silver-enhanced gold nanoparticle label of which detection limit for human IgG is 1.0 ng ml^{-1} (Chu et al., 2005) and comparable with the fluoroimmunoassay of which the detection limit is 0.1 ng ml^{-1} (Evangelista et al., 1991). Since the solution volume for the determination of Ag(I) ions was relatively large in this work, it resulted in the loss of sensitivity on a certain extent. If less volume were applied, by using screen-printed electrode (SPE) for example, further improvement of the sensitivity would be potential. In summary, the proposed ultrasensitive approach holds great promise for the extended application in the field of bioaffinity assays, environmental monitoring, pharmaceutical analysis and clinical diagnosis.

Acknowledgements

The work was financially supported by National Natural Science Foundation of PR China (Grant Nos. 20435010, 20375012, 20205005, and 20675028).

References

Alfonta, L., Bardea, A., Khersonsky, O., Katz, E., Willner, I., 2001. Biosens. Bioelectron. 16, 675–687.
Bakker, E., 2004. Anal. Chem. 76, 3285–3298.

Bakker, E., Qin, Y., 2006. Anal. Chem. 78, 3965–3983.
Bakker, E., Telting-Diaz, M., 2002. Anal. Chem. 74, 2781–2800.
Cai, H., Wang, Y., He, P., Fang, Y., 2002. Anal. Chim. Acta 469, 165–172.
Cao, Y.W.C., Jin, R.C., Mirkin, C.A., 2002. Science 297, 1536–1540.
Chu, X., Fu, X., Chen, K., Shen, G.L., Yu, R.Q., 2005. Biosens. Bioelectron. 20, 1805–1812.
Dequaire, M., Degrand, C., Limoges, B., 2000. Anal. Chem. 72, 5521–5528.
Evangelista, R.A., Pollak, A., Templeton, E.F.G., 1991. Anal. Biochem. 197, 213–224.
Faulk, W.P., Taylor, G.M., 1971. Immunochemistry 8, 1081–1083.
He, L., Musick, M.D., Nicewarner, S.R., Salinas, F.G., Benkovic, S.J., Natan, M.J., Keating, C.D., 2000. J. Am. Chem. Soc. 122, 9071–9077.
Horisberger, M., Rosset, J., Bauer, H., 1975. Experientia 31, 1147–1149.
Hwang, S., Kim, E., Kwak, J., 2005. Anal. Chem. 77, 579–584.
Ipe, B.I., Thomas, K.G., 2004. J. Phys. Chem. B 108, 13265–13272.
Jacobs, 1963. Anal. Chem. 35, 2112–2115.
Katz, E., Alfonta, L., Willner, I., 2001. Sens. Actuators B 76, 134–141.
Katz, E., Willner, I., Wang, J., 2004. Electroanalysis 16, 19–44.
Kokado, A., Arakawa, H., Maeda, M., 2000. Anal. Chim. Acta 407, 119–125.
Liao, K.T., Huang, H.J., 2005. Anal. Chim. Acta 538, 159–164.
Lyon, L.A., Musick, M.D., Natan, M.J., 1998. Anal. Chem. 70, 5177–5183.
Ni, J., Lipert, R.J., Dawson, G.B., Porter, M.D., 1999. Anal. Chem. 71, 4903–4908.
Park, S.J., Taton, T.A., Mirkin, C.A., 2002. Science 295, 1503–1506.
Santos, D.S., Goulet, P.J.G., Pieczonka, N.P.W., Oliveira, O.N., Aroca, R.F., 2004. Langmuir 20, 10273–10277.
Schofield, C.L., Haines, A.H., Field, R.A., Russell, D.A., 2006. Langmuir 22, 6707–6711.
Su, X., Li, S.F.Y., O'Shea, S.J., 2001. Chem. Commun. 8, 755–756.
Taton, T.A., Mirkin, C.A., Letsinger, R.L., 2000. Science 289, 1757–1760.
Wang, J., 1999. Anal. Chem. 71, 328R–332R.
Wang, J., Polsky, R., Xu, D., 2001. Langmuir 17, 5739–5741.
Wang, J., Song, F.Y., Zhou, F.M., 2002. Langmuir 18, 6653–6658.
Wang, J., Liu, G., Jan, M.R., 2004. J. Am. Chem. Soc. 126, 3010–3011.
Zhou, X.C., O'Shea, S.J., Li, S.F.Y., 2000. Chem. Commun. 11, 953–954.